LIMNOLOGY
and
OCEANOGRAPHY: METHODS

Limnol. Oceanogr.: Methods 6, 2008, 208–217

In situ ecosystem-based carbon dioxide perturbation experiments: Design and performance evaluation of a mesocosm facility

Ja-Myung Kim[1], Kyoungsoon Shin[2], Kitack Lee[1], and Byong-Kwon Park[1]*
[1]Pohang University of Science and Technology, School of Environmental Science and Engineering, Pohang, 790-784, Korea
[2]Korea Ocean Research and Development Institute/South Sea Institute, Jangmok, 656-830, Korea

Abstract

We describe a mesocosm facility that can be used for in situ CO_2 perturbation experiments. The facility consists of a floating raft, nine impermeable cylindrical enclosures (each approximately 2400 L in volume), pCO_2 regulation units, and bubble-mediated seawater mixers. Each enclosure is two-thirds filled with seawater, and the headspace above is filled with air at a target pCO_2 concentration. Each enclosure is capped with a transparent dome that transmits incoming radiation. To produce pCO_2 levels higher than the ambient concentration, the mass flow controller in the pCO_2 regulation unit delivers varying amounts (10–320 mL min^{-1}) of ultra-pure CO_2 into the gas mixer where it is rapidly mixed with ambient air (approximately 50 L min^{-1}). To produce pCO_2 levels lower than the ambient concentration, CO_2-free air and ambient air are mixed in the gas mixer. Prior to daily seawater sampling, approximately 0.5 L min^{-1} of the target concentration pCO_2 air stream is diverted to the seawater mixer for thorough mixing with the seawater in the enclosure, while the major fraction of the target concentration pCO_2 air stream continues to flow into the enclosure headspace. A performance evaluation of the mesocosm facility assessed attainment of target pCO_2 concentrations in the headspace and enclosure seawater, and the mixing efficiency of the seawater mixer. The results indicate that the facility is suitable for carrying out in situ pCO_2 perturbation experiments.

Over the past two centuries, the accumulation of fossil-fuel CO_2 in the upper ocean has increased the gaseous CO_2 concentration but decreased pH and the carbonate ion concentration (Feely et al. 2004; Sabine et al. 2004). Consequently, surface water pH is now about 0.1 units lower than it was during the pre-industrial era, and it is predicted to fall by an additional 0.3 units by 2100 (Caldeira et al. 2003). Such a reduction in pH will lead to lowering of the saturation state of seawater with respect to biogenic calcite and aragonite (Feely et al. 2002, 2004; Chung et al. 2003, 2004), and a reduction in the rate of calcium carbonate production in corals (Orr et al. 2005). Changes in ocean carbonate chemistry influence not only sensitive marine ecosystems (e.g., calcifying organisms), but also other interacting components (e.g., preys, predators, and competitors) via changes in nutrient use of phytoplankton and growth rate of heterotrophic organisms. The transfer of these effects through the ecosystem could be either repressed or reinforced, depending on the occurrence of positive or negative feedback loops. Therefore, the mechanisms tending to repress or reinforce the effects of changes in ocean carbonate chemistry should urgently be identified to enable scenarios of future impacts on ecosystem function and biogeochemical cycles to be developed. To gain an integrated understanding of the sensitivity of marine biota to anthropogenic perturbations, there is a particular need for manipulative experiments at the community and ecosystem levels. Such experiments can be undertaken in large enclosures or the open ocean, but enclosed experimental systems enable easy manipulation of experimental conditions and are amenable to a greater degree of replication and repeatability than open ocean experiments (Kemp et al. 1980; Kareiva 1989).

The response of the marine ecosystem to fossil-fuel CO_2 and associated biogeochemical feedback processes has been investigated in a series of mesocosm-based experiments (Engel et al. 2004; Rochelle-Newall et al. 2004; Engel et al. 2005; Grossart et al. 2006; Kim et al. 2006). Two major mesocosm facilities used in these experiments have proved useful for in situ pCO_2 manipulation experiments. Of these, the

*Corresponding author. Phone: 82-54-279-2285; fax: 82-54-279-8299; e-mail: ktl@postech.ac.kr

Acknowledgments

The paper benefited a great deal from the numerous constructive suggestions by two anonymous reviewers and Dr. John Smol. Discussions with Dr. Ulf Riebesell were extremely helpful in the early stage of developing the mesocosm facility. This work was financially supported by the National Research Laboratory (NRL) Program of the Korea Science and Engineering Foundation. Partial support was also provided by the AEBRC at POSTECH.

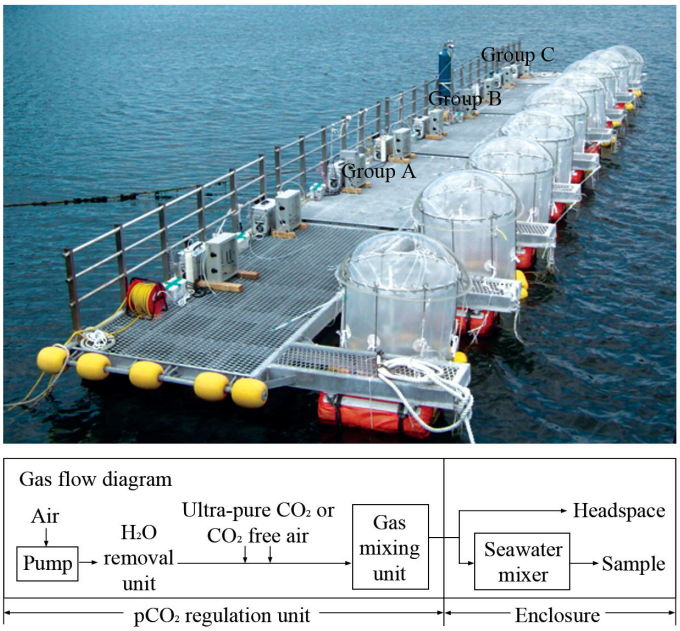

Fig. 1. Photograph of the floating raft, pCO_2 concentration regulation units, and enclosures of the mesocosm facility. The lower diagram shows the pathways of target pCO_2 air generated from a pCO_2 regulation unit to an enclosure.

European Union Large Scale Facility (LSF) in Bergen, Norway, was used in most of mesocosm studies noted above. It consists of nine polyethylene gas-tight enclosures (5 m in height and 2 m in diameter, a total volume of ~11 m^3). Air with the target pCO_2 concentration, produced by mixing ambient air with high pCO_2 air or CO_2-free air, is introduced into the enclosure headspace to maintain the target concentration, and into an air-lifting device for mixing with seawater (Williams and Egge 1998; Engel et al. 2005).

The design and performance of the above mesocosm facility have yet to be described in detail and assessed. In the present study, we evaluated the performance, over a wide range of experimental conditions, of a pCO_2 regulation unit and a bubble-mediated seawater mixer, both of which are key components of our mesocosm facility. We document the optimal operational settings that ensure generation of the target pCO_2 concentrations in the headspace and enclosure seawater and show that the experimental setup enhances the homogeneity of seawater and causes minimal disturbance of planktonic organisms.

Materials and methods

Description of the components of the CO2 mesocosm facility—Our CO_2 mesocosm facility is located at Jangmok (34.6°N and 128.5°E) on the southern coast of Korea. The facility consists of a floating raft, nine impermeable enclosures with transparent caps, nine pCO_2 regulation units, and nine bubble-mediated seawater mixers. Fig. 1 shows the configuration of the major components of the facility.

Floating raft—The raft (approximately 19 m long and 3 m wide) is constructed from steel frames and mounted on rubber floats anchored to the sea floor approximately 50 m seaward of a pier. The nine enclosures are moored to the floating raft and aligned perpendicular to the sun's pathway to ensure that all receive approximately the same intensity of solar radiation. The average water depth beneath the raft is 5 m on the ebb tide and 9 m on the flood tide.

Impermeable enclosures with transparent caps—The enclosures are cylindrical (3 m in height, 1 m in diameter) and made of polyethylene. Approximately the top 1 m of each enclosure is above the water surface to prevent the accidental incursion of seawater due to wave action. The top of each enclosure is covered with a hemisphere-shaped acryl cap (approximately 1.2 m in diameter and 0.4 m in height) that is transparent to solar radiation. The gap between the enclosure and the cap is less than 1 cm.

pCO_2 concentration-regulation units—The pCO_2 regulation units were designed to generate air with a wide range of pCO_2 concentrations and to dispense the air to enclosure headspaces and seawater. The pCO_2 target values were 280, 390, and 950 μatm, representing the pre-industrial, present-day, and predicted year 2100 atmospheres, respectively. The pCO_2 value of 950 μatm for the year 2100 was based on model projections using one of the Intergovernmental Panel on Climate Change's emission scenarios (A1FI; Houghton et al. 2001). Each of the target pCO_2 concentration air masses was produced by three replicate pCO_2 regulation units. All nine pCO_2 regulation units were separately encased in stainless steel panels (36 cm wide, 15 cm long, and 40 cm high), the surfaces of which were anodized to prevent rusting associated with the deposition of sea salts. The main components of the pCO_2 regulation units (Fig. 2) are described in details in the following sections.

Air pumps—A gas flow sufficient to flush the 1000 L enclosure headspace, maintain the target pCO_2 concentration in the headspace, and maintain flow into the seawater mixer requires a considerable gas flow rate. A further consideration is the air pump emitting pressure. For normal operation of a static gas mixer (see Fig. 3), emitting pressures greater than 1 kPa are required. Oil-less rocking piston air pumps (75R645–P101– H302X; GAST, USA) were chosen to meet these requirements. Each pump is 24 cm wide × 9 cm long × 19 cm high, weighs approximately 8 kg, and can generate an air flow rate of approximately 140 L min^{-1} and a maximum pressure of 2 kPa in open flow mode. In the mesocosm configuration, the pumps produce an air-flow rate of 50 L min^{-1} and air pressure of approximately 1 kPa. These reductions in efficiency are probably caused by resistance in the gas lines and controlling valves installed along the lines.

Water vapor removal units—We cool the hot air (>80°C) emitted by the air pumps by forcing it through a submerged stainless steel fiber-coated Teflon line. The cooled air then passes through an air filter (AF320-10; Parker) for collection of condensed water in a drain pot. To enable further drying, the

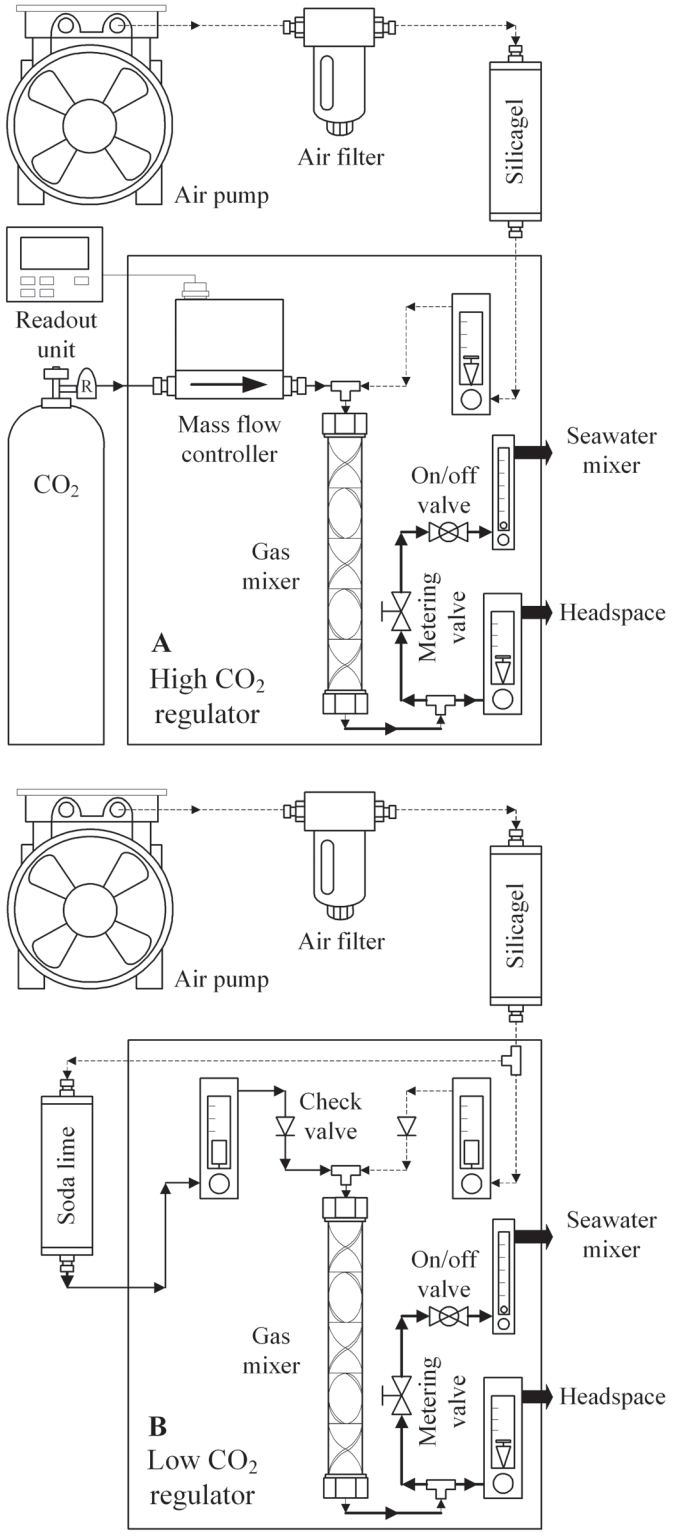

Fig. 2. Diagrams of two different pCO_2 regulation units. (A) Unit for producing pCO_2 concentrations higher than the ambient value. (B) Unit for producing pCO_2 concentrations lower than the ambient value. The dashed and thin solid lines in (A) and (B) indicate pathways of ambient air and pure CO_2 (or CO_2-free air), whereas the thick solid lines indicate pathways of target pCO_2 air.

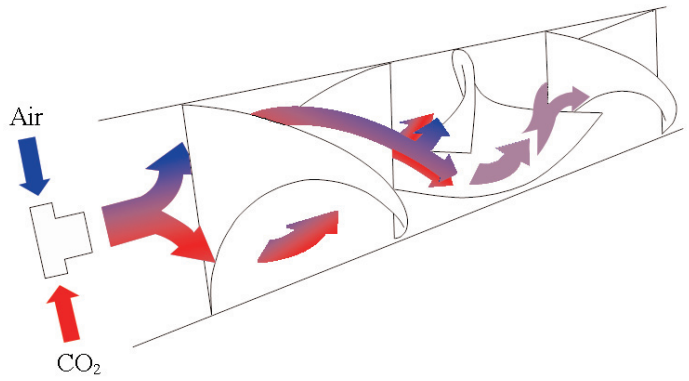

Fig. 3. A conceptual diagram of gas mixing within a static gas mixer. Blue and red arrows indicate streams of ambient air and ultra-pure CO_2, respectively. Purple arrows indicate bisection and mixing of the gases by the plates.

air is passed through silica gel (3 mm particle size) in an acryl tube (8 cm diameter and 40 cm long) with screw caps at both ends. The silica gel is replaced approximately every 10 h when used under the standard air-flow rate. Both an air filter and a desiccant tube are installed upstream of the pCO_2 regulation unit to avoid malfunction of the unit due to condensation.

Gas-mixing units—Each gas-mixing unit consists of a ball flow meter (060801-227, 060710-161, 060801-222; KOFLOC, Japan), a mass flow controller (3660; KOFLOC, Japan), and a static gas mixer (T6-15-21; Noritake, Japan). The mass flow controller accurately delivers ultra-pure (99.999%) CO_2 at varying rates (from 10 to 320 mL min^{-1}) into the gas mixer where the CO_2 is thoroughly mixed with ambient air at a high flow rate controlled by a ball flow meter. The real-time flow rate of the ultra-pure CO_2 stream can be read from a readout box.

The static gas mixer is a key component of these gas-mixing devices and is housed in a thin-walled tube for bite-type fitting (Fig. 2). The mixers have an internal diameter of 11 mm and are 26 cm in length. Each mixer contains 15 rectangular plates (1.5 times their internal diameter) twisted at 180° and aligned alternately at an angle of 90°. Both the ultra-pure CO_2 and ambient air streams simultaneously flow into a T-shaped connector within which both gases are roughly mixed. For more thorough mixing, the gas mixture subsequently flows into the first plate within which the gas mixture is bisected. As the bisected gas streams enter the second plate, they merge and the stream is then bisected again into two new gas streams (Fig. 3). By repeating this process 15 times, the small amount of added ultra-pure CO_2 is mixed thoroughly and rapidly with the ambient air. According to the direction of the twist, the gas streams are rotated either toward the pipe wall or to the center. This configuration facilitates thorough mixing of the gases by creating a strong flow-reversal motion. This gas mixer enables generation of target pCO_2 levels to be achieved that are either higher or lower than the ambient level.

Generating pCO_2 levels that exceed ambient concentrations—The pCO_2 gas regulation unit shown in Fig. 2A produces air with pCO_2 levels higher than the ambient concentration (approximately 390 μatm). Simultaneous entry of ambient air and ultra-pure CO_2 to a static mixer at flow rates of 50 L min^{-1} and 40 mL min^{-1}, respectively, generates air with a pCO_2 value of approximately 950 μatm. A minimum tank pressure of 2.5 kPa in the ultra-pure CO_2 tank is needed to generate a flow rate of 40 mL min^{-1}.

Generating pCO_2 levels below ambient concentrations—The pCO_2 regulation unit shown in Fig. 2B produces air with pCO_2 levels lower than the ambient concentration by mixing ambient air and CO_2-free air. To produce CO_2-free air the ambient air stream is passed at a rate of approximately 20 L min^{-1} through a desiccant tube (8 cm diameter, 40 cm long) containing 1.5 kg of Na_2CO_3 platelet crystals. The pCO_2-free and ambient air streams are directed concurrently into the gas mixer at equivalent flow rates of approximately 20 L min^{-1}.

Generating ambient pCO_2 levels—The chosen pump directly delivers ambient air into the headspaces of each enclosure, and the seawater mixer housed therein.

Seawater mixers—Previous studies used air lifting (Engel et al. 2005) and mechanical stirring (Alldredge et al. 1995) to mix seawater within enclosures. In our mesocosm system, we use two acryl pillars installed in each enclosure to gently aerate the seawater with air at the target pCO_2 concentration to ensure the homogeneous distribution of phytoplankton and solutes. Each seawater mixer consists of two pillars (15 cm diameter and 1.8 m high) 50 cm apart and attached to individual vertical poles for support (Fig. 4). Each mixing unit has two spare supporting poles for additional pillars. All these components are supported by polypropylene rings (approximately 80 cm diameter), one each at the top, in the middle, and at the bottom (Fig. 4). Bubbles in each pillar are generated by a bubble stone (11 cm diameter; S104-B; SUDO, Japan) located approximately 50 cm above the bottom of the pillar. As fine bubbles from the bubble stone push seawater from the lower part of the enclosure to the surface, outside seawater is introduced into the pillar through holes just below the bubble stone. Consequently, incoming seawater is continuously transferred to the surface by rising bubbles. This mixing scheme generates a convective flow of seawater within the enclosure that enhances the homogeneity of the seawater in terms of phytoplankton cell density and solute concentration.

Sequence of the mesocosm setup—Following introduction of seawater into the enclosures, the target pCO_2 concentration in the enclosed seawater is usually attained within a day using the pCO_2 regulation units. After adjusting the seawater pCO_2, target concentration pCO_2 air mass is pumped only into the enclosure headspace for the duration of the experiment. For 20 min per day, a small fraction (approximately 0.5 L min^{-1}) of this air is diverted into the seawater mixer, while the major fraction (approximately 49.5 L min^{-1}) continues to flow into the enclosure headspace. Immediately after 20 min, seawater aeration is completed the enclosures are sampled. This dichotomous gas flow scheme significantly reduces seawater sampling bias while maintaining the target pCO_2 value in the headspace.

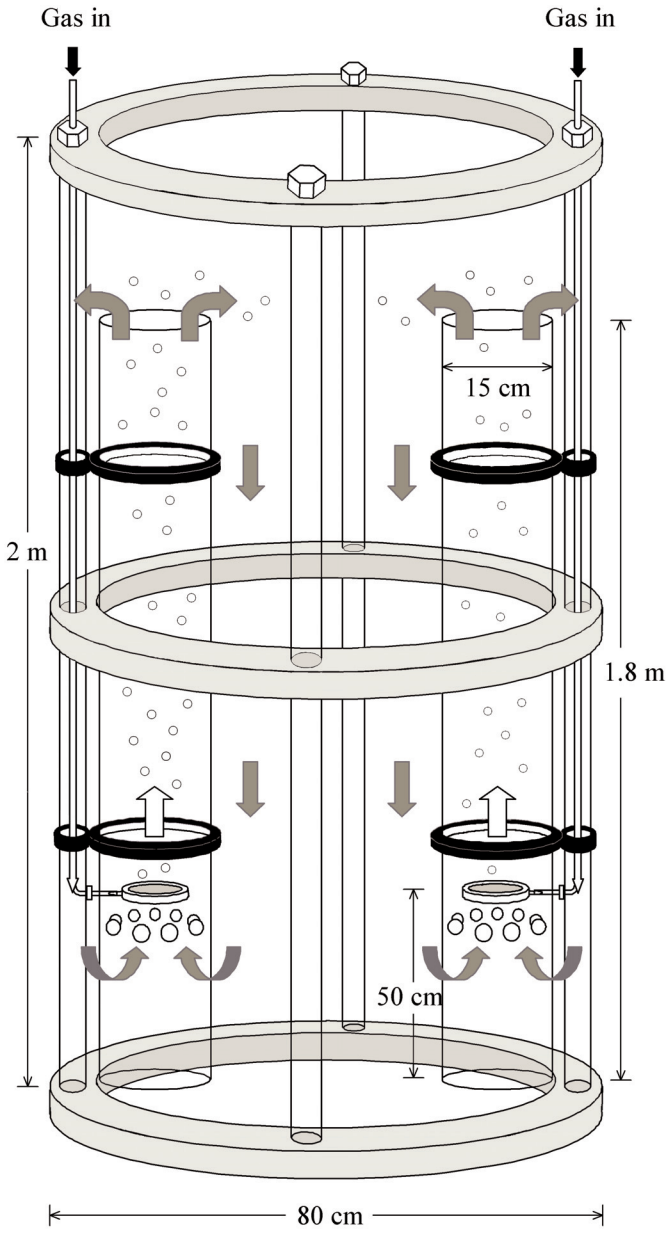

Fig. 4. Schematic diagram of an acryl pillar-type seawater mixer. Polypropylene rings (gray) are installed at the top, middle, and bottom. Gray arrows indicate the direction of water flow, while the small black arrows indicate the direction of gas flow.

Assessment

Generation of target pCO_2 concentrations using the pCO_2 concentration regulation units—The performance of our pCO_2

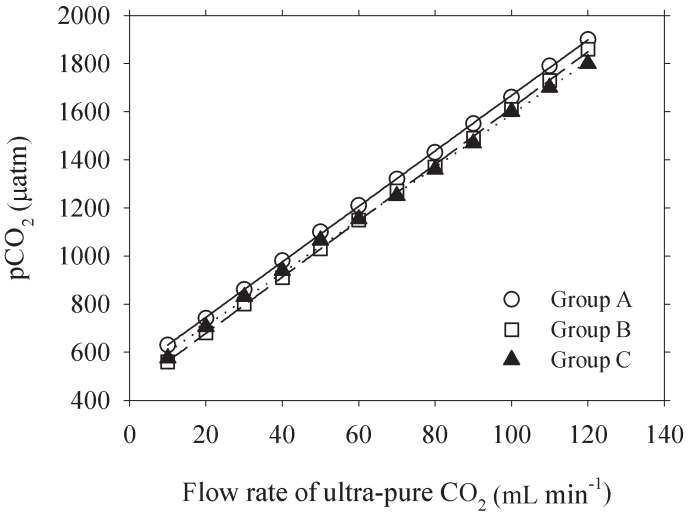

Fig. 5. pCO_2 concentrations as a function of the rate of ultra-pure CO_2 added into a static gas mixer into which a constant rate of ambient air (50 L min^{-1}) was simultaneously added. Circles, squares, and triangles denote the three different pCO_2-regulation units employed in Groups A, B, and C, respectively.

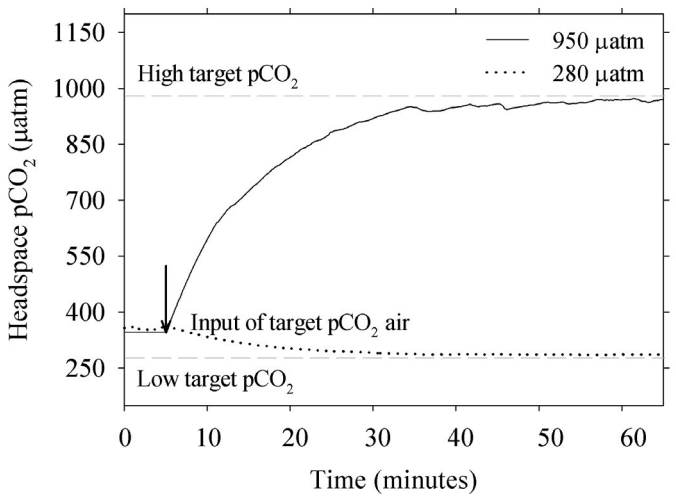

Fig. 6. Measured pCO_2 concentrations in the headspaces of the enclosures treated with 950 µatm pCO_2 air (solid line) and 280 µatm pCO_2 air (dotted line) over 1 h.

regulation unit was assessed by measuring the degree to which resulting pCO_2 concentrations coincided with target pCO_2 levels (280 to 950 µatm). In particular, the resulting pCO_2 levels were sensitive to the ratio of ultra-pure CO_2 and ambient air entering the gas mixers: the higher the gas mixing ratios the higher the resulting pCO_2 concentrations. For example, we varied the flow rate of ultra-pure CO_2 between 10 and 120 mL min^{-1} while maintaining a constant flow rate (50 L min^{-1}) of ambient air. The pCO_2 concentrations of the resulting air were measured using an infrared analyzer (Li–Cor 820), and showed a linear trend with increasing release rates of ultra-pure CO_2 (Fig. 5). For the three pCO_2 regulation units tested, the increase in pCO_2 as a function of the rate of ultra-pure CO_2 added was nearly identical.

Regulation of target pCO_2 concentrations in enclosure headspaces—We continuously monitored the pCO_2 concentrations in the headspaces of two enclosures to assess how quickly the target pCO_2 value was reached and whether it could be maintained (Fig. 6). To maintain the target value, the enclosure headspaces were largely isolated from the outside atmosphere and were continuously flushed with 50 L min^{-1} of air flow. Immediately following input of target pCO_2 air into the enclosure headspaces, we sampled air from approximately 20 cm above the air-water interface within the enclosures. The target pCO_2 concentration was achieved within 30 min of input of the target pCO_2 air and was maintained at 958 ± 10 µatm thereafter (Fig. 6). Under the wind speed condition (2–6 m s^{-1}) at which this experiment was undertaken, the target pCO_2 value remained approximately unchanged with only minor fluctuations. The tightly closed enclosure-cap system ensures a stable concentration of pCO_2 in the headspace. With the gas regulation unit in the described configuration, the lowest achievable pCO_2 concentration within the headspace was approximately 287 ± 5 µatm (Fig. 6), which is comparable to the pCO_2 value during the pre-industrial period.

Generation of target pCO_2 concentrations in enclosure seawater—Immediately after adding seawater to the enclosures, we bubbled pCO_2-free air into one set of three enclosures at a rate of approximately 0.5 L min^{-1}, to generate a target seawater pCO_2 level (280 µatm) below the ambient level. We also bubbled air with a pCO_2 level four times the target concentration into another set of three enclosures to achieve a seawater pCO_2

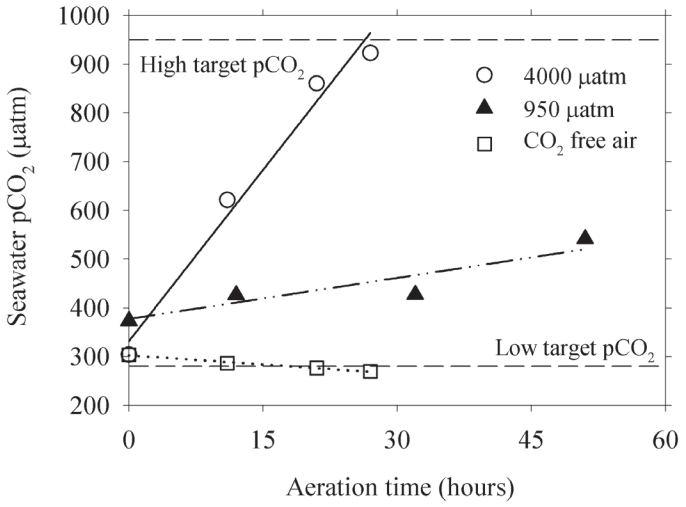

Fig. 7. Seawater pCO_2 concentrations in the enclosures as a function of aeration time. Circles, triangles, and squares represent aeration with 4000 µatm, 950 µatm, and 0 µatm pCO_2 air, respectively.

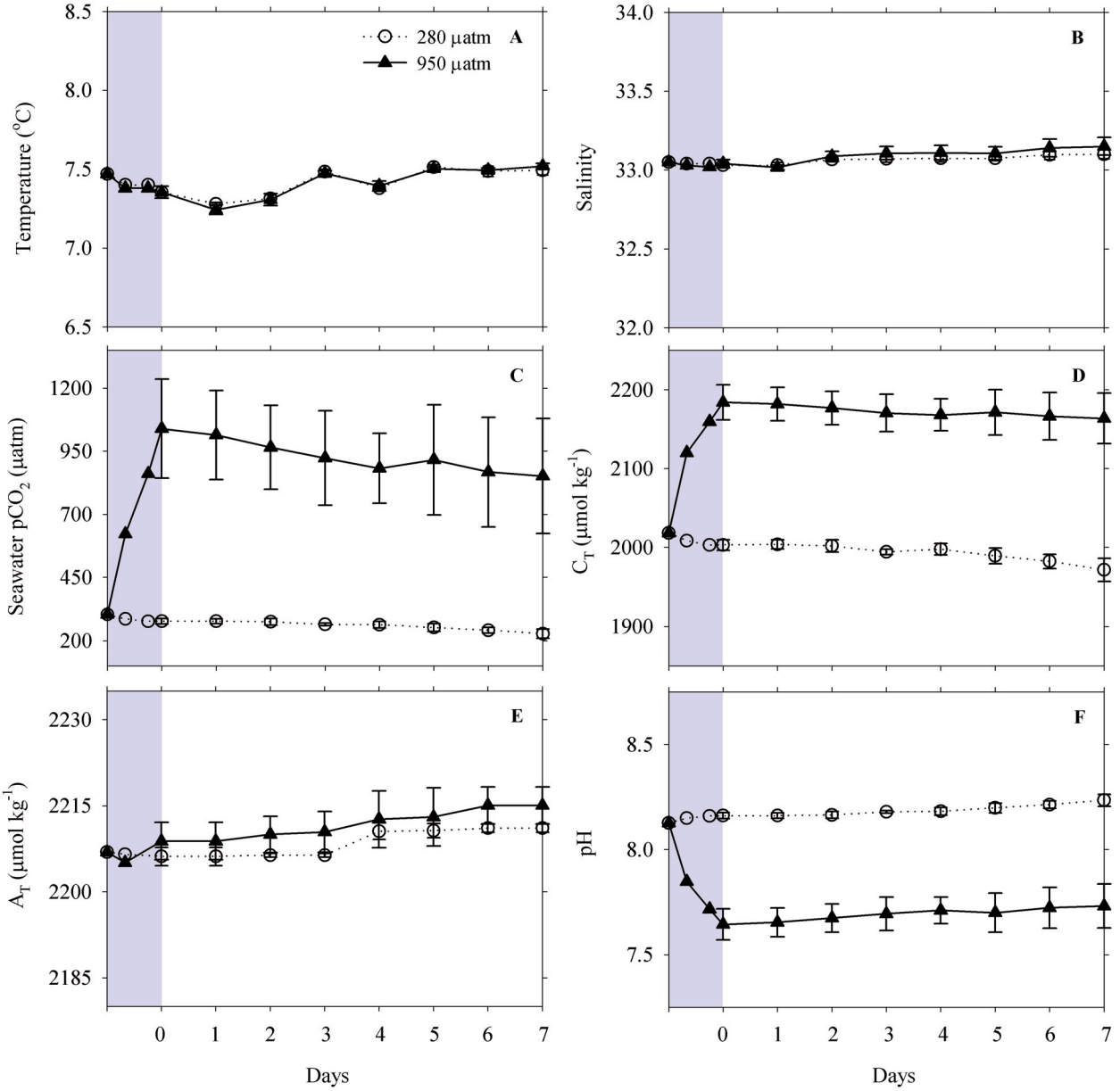

Fig. 8. Changes in (A) temperature, (B) salinity, (C) pCO_2, (D) total dissolved inorganic carbon (C_T), (E) total alkalinity (A_T), and (F) pH in enclosure seawater over an 8-d period that includes the 1-d aeration period. The headspaces of the two enclosures were continuously filled (from Day 0 to Day 7) with pCO_2 values of 280 µatm (open circles) or 950 µatm (filled triangles) pCO_2. The shaded bars represent the 1-d aeration period during which either pCO_2-free or 4000 µatm pCO_2 air were bubbled into the enclosure sweater to adjust the seawater pCO_2 to the target values of 280 µatm and 950 µatm, respectively. Error bars represent the standard deviations of the mean results of the replicate enclosures.

level of 950 µatm. This enabled us to assess changes in seawater carbonate parameters in enclosures with target pCO_2 levels of 280 µatm and 950 µatm. The bubbling rate was sufficiently gentle to cause minimal impact on the phytoplankton assemblage. Using this pCO_2 manipulation method, seawater pCO_2 levels in the enclosures attained the target concentrations within 24 h (Fig. 7, and the shaded bar in Fig. 8C). The slopes of the best-fit trends relating the aeration time and the pCO_2 concentration in seawater samples differed significantly, depending on the pCO_2 concentration in the injected air: 23.4 (r^2 = 0.9794) for 4000 µatm and 2.9 (r^2 = 0.8484) for 950 µatm. The seawater pCO_2 concentrations were not measured directly because the protocol for using an infrared analyzer/equilibrator-based pCO_2 system involves removal of phytoplankton from the seawater. Consequently, calculations of the seawater pCO_2 (and pH) levels in the enclosures were based on measurements of total dissolved inorganic carbon (C_T) and total alkalinity (A_T) of the samples using the carbonic acid dissociation constants

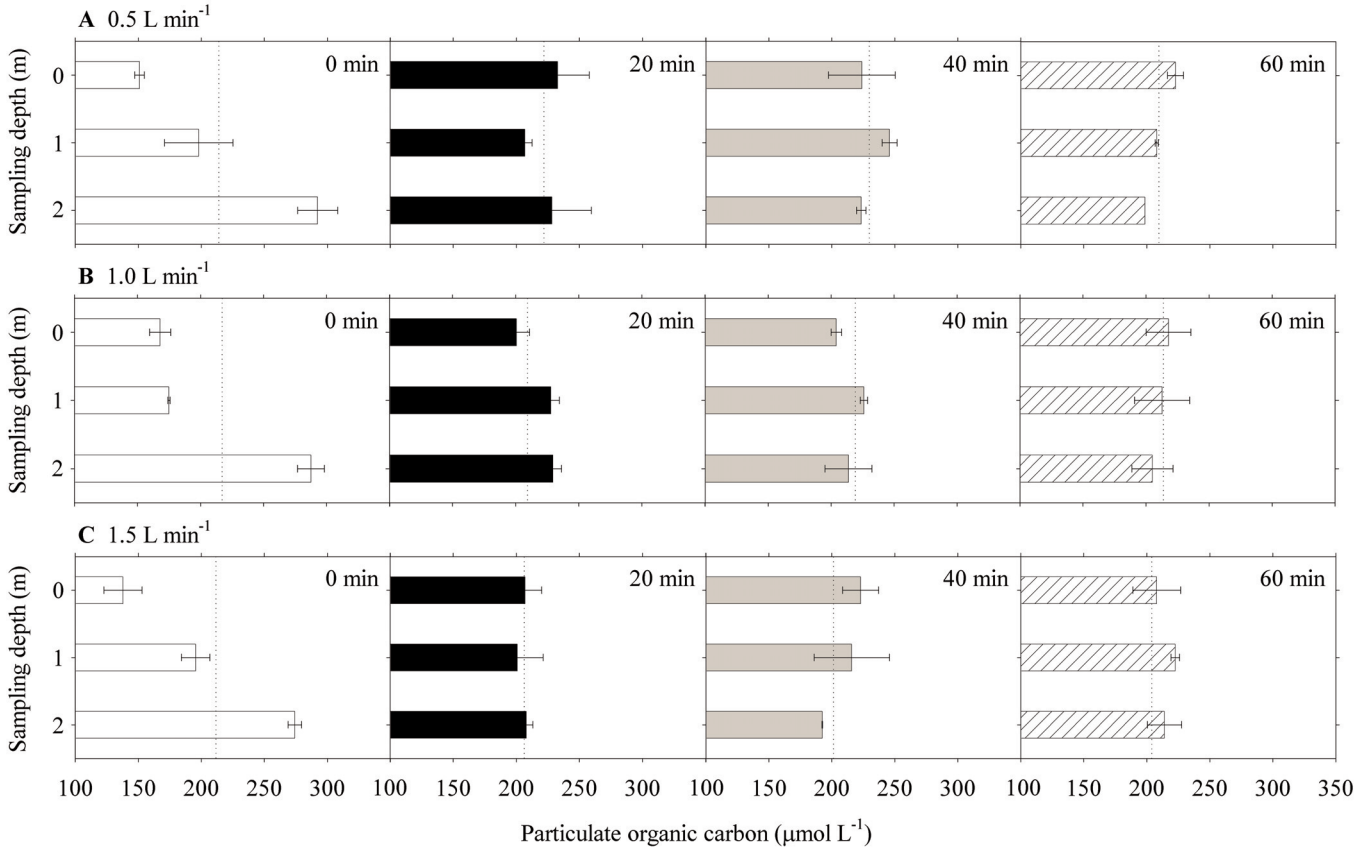

Fig. 9. Particulate organic carbon concentrations as a function of three sampling depths (0 m, 1 m, and 2 m) with different bubbling gas flow rates: (A) 0.5 L min^{-1}, (B) 1.0 L min^{-1}, and (C) 1.5 L min^{-1}. Different colored bars represent different mixing times from 0 min to 60 min. Dashed line represents the average value of POC in three depths.

of Mehrbach et al. (1973) that were refitted in different functional forms by Dickson and Millero (1987). This set of thermodynamic constants has proved to be the most consistent with laboratory (Lee et al. 1996; Lueker et al. 2000; Mojica Prieto and Millero 2002; Millero et al. 2006) and field (Lee et al. 1997, 2000; Wanninkhof et al. 1999; Millero et al. 2002) measurements of carbon parameters over the oceanic ranges of temperature and salinity. Given the uncertainty (± 2 μmol kg^{-1}) in C_T and A_T measurements, the predicted pCO_2 and pH values based on C_T and A_T were accurate to ± 5 μatm and ± 0.005 units, respectively. To monitor changes in seawater pCO_2 levels in the enclosures, it is recommended that measurements of C_T and A_T be performed approximately daily over the duration of mesocosm experiments.

The bubbling procedure changed the seawater carbonate chemistry without changing the seawater temperature or salinity. The temperature (7.4 ± 0.1°C) and salinity (33.0 ± 0.01) of seawater in the enclosures were approximately constant for the initial 24-h period (the shaded bars in Figs. 8A and 8B). The target pCO_2 level determined the degree of change in pH and C_T. For example, there was a 150 μmol kg^{-1} increase in C_T concentration in the enclosure with a target pCO_2 concentration of 950 μatm, whereas there was a 21 μmol kg^{-1} decrease in C_T concentration in the enclosure with a target pCO_2 concentration of 280 μatm (the shaded bar in Fig. 8D). As expected, A_T remained unchanged with addition of air at the target pCO_2 concentration (the shaded bar in Fig. 8E). The calculated pH decreased by approximately 0.44 units in enclosures with a target pCO_2 concentration of 950 μatm, but increased slightly (0.04 units) in enclosures with a target pCO_2 concentration of 250 μatm (the shaded bar in Fig. 8F).

We also monitored changes in seawater carbonate parameters over the 7-d period after seawater pCO_2 in the two enclosures reached the target levels (Day 0 through Day 7, Fig. 8). Seawater pCO_2 and C_T in the enclosures gradually decreased due to biological activity, which also had the effect of increasing seawater pH. The A_T in seawater increased slightly (5–6 μmol kg^{-1}) in the two treatments due to evaporation-induced salinity increase. The magnitudes of the reductions in pCO_2 and C_T observed during the experiment were lower than expected, due to the flux of CO_2 from the mesocosm atmosphere.

Evaluation of the degree of homogeneity of seawater samples—To determine the optimal aeration rate and time to minimize the standard deviation of the measured particulate organic carbon (POC) concentrations, we aerated the seawater at three different gas flow rates: 0.5, 1.0, and 1.5 L min^{-1}. We then took duplicate samples from each of the surface, middle, and lower (the depth at which the bubble stone was installed) parts of an enclosure at each of four different stages: prior to aeration, and at 20, 40, and 60 min after aeration was initiated. In the absence of seawater, mixing the POC concentrations were highest in samples taken from the lower parts of the enclosure (Fig. 9). This probably reflects the accumulation of organic matter by settlement.

Variations in POC concentration with depth was significantly reduced in samples taken 20 min after initiation of aeration (Fig. 10). In particular, the standard deviation from the average of the six POC concentrations decreased significantly, from 30% prior to aeration to less than 10% at 20 min after aeration was initiated, regardless of the aeration flow rates. The results of this experiment indicate that the degree of homogeneity of seawater samples was optimized within 20 min of aeration with an aeration flow rate of 0.5 L min^{-1}.

It is also important to note that the 20 min aeration process affected seawater pCO_2 concentrations to a minor degree; for example, for 950 μatm pCO_2 air the pCO_2 concentration in seawater increased by less than a few micro-atmospheres. This elevation in seawater pCO_2 was predicted from the equation relating aeration period and seawater pCO_2 concentration, shown in Fig. 7.

Evaluation of initial phytoplankton composition after filling the enclosures with seawater—After filling all enclosures with seawater, we assessed phytoplankton composition across the nine enclosures. The mean phytoplankton concentration (>10 μm) in the nine enclosures was 278,030 ± 84,020 cells L^{-1}. The relative abundances of the two major phytoplankton species *Eutreptiella gymnastica* and *Skeletonema costatum* were similar across the nine enclosures (Fig. 11). Their combined populations accounted for approximately 95% of the population in all but one enclosure (C1) (Fig. 11). Of the two main species, *E. gymnastica* was by far the major component, accounting for approximately 84% ± 7% when averaged over all nine enclosures.

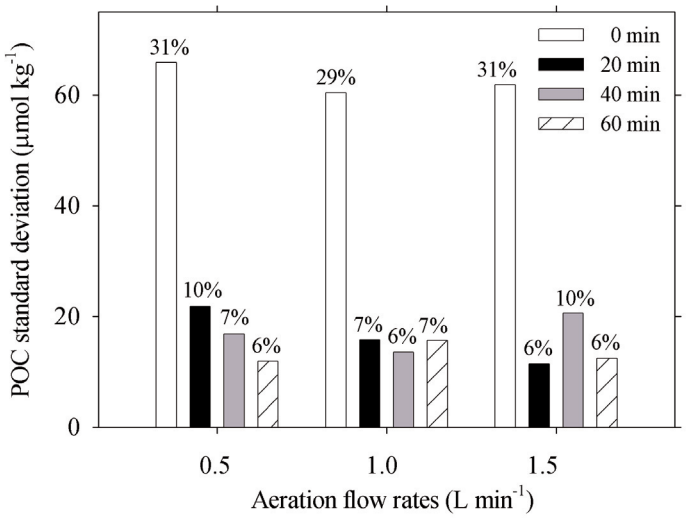

Fig. 10. Standard deviations (%) from the average values of the six particulate organic carbon concentrations (POC) as a function of the duration of aeration prior to seawater sampling. Sampling was performed in duplicates from each of the surface, middle and lower parts of the enclosure.

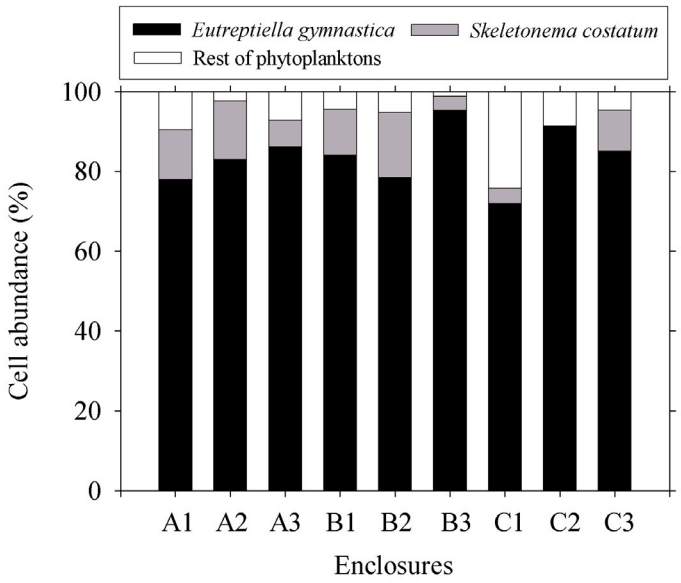

Fig. 11. Relative contributions (%) of the two major phytoplankton populations to the total phytoplankton cell density in nine enclosures after dispensing the seawater. The letters A, B, and C refer to three different groups of enclosures, and the numbers refer to the three enclosures treated with the same pCO_2 air.

Discussion

We report the design of a mesocosm facility that was established and thoroughly tested at Jangmok (34.6°N and 128.5°E), on the southern coast of Korea. The fully automated pCO_2-controlling system consistently and accurately delivered air to the headspaces and seawater in enclosures at pCO_2 concentrations covering the range from pre-industrial to projected year 2100 atmospheres. The seawater mixing device gently and thoroughly mixed seawater in the enclosures within 20 min of addition, and with minimal perturbation. Performance evaluations indicated that the mesocosm facility is suitable for in situ experiments that involve testing of the short-term effects (approximately 30 d) of pCO_2 on a marine ecosystem. The proposed duration of mesocosm experiments is sufficiently long to observe impacts of seawater pCO_2 concentration changes on relatively sensitive ecosystem processes, such as the calcification rates of calcifying organisms (Engel et al. 2005) and growth rates of diatom species (Kim et al. 2006). Other important

scientific questions that need to be addressed include the effects of seawater pCO_2 concentration on carbon export production and shifts in phytoplankton species composition. Future studies should also focus on assessing the reliability (including the experimental duration) of mesocosm-based manipulative studies, in particular their adequacy for addressing these urgent scientific issues.

Although our mesocosm facility emulated the oceanic environment, the design of the system produces three artifacts. First, as with other mesocosm-based studies, these studies are inadequate for assessing the chronic effects of CO_2 perturbations because of wall effects and deviations of the plankton community within the enclosures from the nearby natural system. Second, phytoplankton within the enclosures are unlikely to experience natural levels of physical turbulence that occur in the ocean. Third, experiments that exclude higher trophic levels provide no insight into the potential effects on phytoplankton growth of interactions between phytoplankton and zooplankton, of organisms of other trophic levels. However, mesocosm experiments could be performed with natural plankton assemblages, without the preferential removal of higher trophic levels.

Despite their limitations, in situ mesocosm pCO_2 manipulation studies provide an effective tool for unravelling the effects of projected future forcing on natural aquatic ecosystems, and provide a link between in vitro experiments and field observations. As human-induced climatic change continues to alter marine environmental conditions, manipulative experiments ranging from the community level to the scale of entire ecosystems will become increasingly relevant.

Comments and recommendations

Many minor factors can collectively affect the success of CO_2 manipulation experiments using a mesocosm facility. Here, we make recommendations regarding three major operational factors that are critical in obtaining significant and reproducible results in mesocosm experiments.

The first is ensuring that all enclosures are leak-proof prior to setting up a mesocosm facility. To check for leaks, we lifted each enclosure using a crane and filled it with approximately 250 L tap water. We then laid the enclosure on a dry floor and, paying particular attention to joins, rolled it to detect leaks. If found, these were carefully sealed using silicon glue. The leak test should be repeated for each enclosure until all leaks are eliminated.

The second concerns the method of dispensing seawater into the enclosures. To increase the homogeneity of phytoplankton composition in enclosure seawater, it is strongly recommended that all enclosures are filled simultaneously with seawater at an identical flow rate. In our experiment, all nine enclosures were positioned in a row close to the mesocosm raft. Garden hoses connected each enclosure to a faucet installed near the bottom of a 2000 L seawater tank, which was filled with seawater pumped from approximately 4 m depth from a site adjacent to the raft and filtered through a 100 µm pore-sized filter before entering the tank. This procedure is likely to increase the probability that the initial composition of the phytoplankton community is similar across all enclosures (see Fig. 11). During the present study period, the bay water was vertically homogenous in terms of physical and chemical parameters, because of winter advective mixing.

The third factor concerns rapidly achieving the target pCO_2 levels in seawater in the enclosures. To achieve pCO_2 levels lower than the ambient concentration, we aerated seawater with pCO_2-free air, while for pCO_2 levels above ambient we aerated the seawater using air with pCO_2 levels that were four-times higher than the target pCO_2 concentration. This aeration protocol meant that seawater samples within all enclosures attained the target pCO_2 levels within about 24 h (Fig. 7).

References

Alldredge, A. L., C. Gotschalk, U. Passow, and U. Riebesell. 1995. Mass aggregation of diatom blooms – Insights from a mesocosm study. Deep-Sea Res. II 42(1): 9–27.

Caldeira, K., and M. E. Wickett. 2003. Anthropogenic carbon and ocean pH. Nature 425:365.

Chung, S. –N., and others. 2003. Calcium carbonate budget in the Atlantic Ocean based on water column inorganic carbon chemistry. Glob. Biogeochem. Cycles. 17(4):doi:10.1029/2002GB002001

———, G. –H. Park, K. Lee, R. M. Key, F. M. Millero, R. A. Feely, C. L. Sabine, and P. G. Falkowski. 2004. Postindustrial enhancement of aragonite undersaturation in the upper tropical and subtropical Atlantic Ocean: The role of fossil fuel CO_2. Limnol. Oceanogr. 49(2):315–321.

Dickson, A. G., and F. J. Millero. 1987. A comparison of the equilibrium constants for the dissociation of carbonic acid in seawater media. Deep-Sea Res. I. 34:1733–1743.

Engel, A., B. Delille, S. Jacquet, U. Riebesell, E. Rochelle-Newall, A. Terbruggen, and I. Zondervan. 2004. Transparent exopolymer particles and dissolved organic carbon production by *Emiliania huxleyi* exposed to different CO_2 concentrations: a mesocosm experiment. Aquat. Microb. Ecol. 34(1):93–104.

——— and others. 2005. Testing the direct effect of CO_2 concentration on a bloom of the coccolithophorid *Emiliania huxleyi* in mesocosm experiments. Limnol. Oceanogr. 50(2): 493–507.

Feely, R. A., and others. 2002. In situ calcium carbonate dissolution in the Pacific Ocean. Glob. Biogeochem. Cycles. 16(4):doi:10.1029/2002GB001866.

———, C. L. Sabine, K. Lee, W. Berelson, J. Kleypas, V. J. Fabry, and F. J. Millero. 2004. Impact of anthropogenic CO_2 on the $CaCO_3$ system in the oceans. Science 305:362–366.

Grossart, H. –P., M. Allgaier, U. Passow, and U. Riebesell. 2006. Testing the effect of CO_2 concentration on the dynamics of marine heterotrophic bacterioplankton. Limnol. Oceanogr. 51(1): 1–11.

Houghton, J. T., Y. Ding, D. J. Griggs, M. Noguer, P. J. Vander Linden, and D. Xiaosu. 2001. Climate change 2001: The scientific bases. Cambridge Univ. Press.

Kareiva, P. 1989. Renewing the dialogue between theory and experiments in population ecology, pp. 68-88. *In* J. Roughgarden et al. [eds.], Perspectives in ecological research. Princeton Univ. Press.

Kemp, W. M., M. R. Lewis, F. F. Cunningham, J. C. Stevenson, and W. R. Boynton. 1980. Microcosms, macrophytes, and hierarchies: environmental research in the Chesapeake Bay, pp. 911-936. *In* J. P. Giesy [eds.], Microcosms in ecological research. National Technical Information Service.

Kim, J.-M., and others. 2006. The effect of seawater CO_2 concentration on growth of a natural phytoplankton assemblage in a controlled mesocosm experiment. Limnol. Oceanogr. 51(4):1629–1636.

Lee, K., F. J. Millero, and D. M. Campbell. 1996. The reliability of the thermodynamic constants for the dissociation of carbonic acid in seawater. Mar. Chem. 55:233–245.

———,———, and R. Wanninkhof. 1997. The carbon dioxide system in the Atlantic Ocean. J. Geophys. Res. 102: 15693–15707.

———, ———, R. H. Byrne, R. A. Feely, and R. Wanninkhof. 2000. The recommended dissociation constant for carbonic acid in seawater. Geophys. Res. Lett. 27(2):229–232.

Lueker, T. J., A. G. Dickson, and C. D. Keeling. 2000. Ocean pCO_2 calculated from dissolved inorganic carbon, alkalinity, and equations for K_1 and K_2: validation based on laboratory measurements of CO_2 in gas and seawater at equilibrium. Mar. Chem. 70:105–119.

Mehrbach, C., C. H. Culberson, J. E. Hawley, and R. M. Pytkowicz. 1973. Measurement of the apparent dissociation constants of carbonic acid in seawater at an atmospheric pressure. Limnol. Oceanogr. 18:897–907.

Millero, F. J., D. Pierrot, K. Lee, R. Wanninkhof, R. Feely, C. L. Sabine, R. M. Key, and T. Takahashi. 2002. Dissociation constants for carbonic acid determined from field measurements. Deep-Sea Res. I. 49:1705–1723.

———, T. B. Graham, F. Huang, H. Bustos-Serrano, and D. Pierrot. 2006. Dissociation constants of carbonic acid in seawater as a function of salinity and temperature. Mar. Chem. 100: 80–94.

Mojica Prieto, F. J., and F. J. Millero. 2002. The values of pK_1 + pK_2 for the dissociation of carbonic acid in seawater. Geochim. Cosmochim. Acta. 66:2529–2540.

Orr, J. C., and others. 2005. Anthropogenic ocean acidification over the twenty-first century and its impact on calcifying organisms. Nature 437:681-686.

Rochelle-Newall, E., and others. 2004. Chromophoric dissolved organic matter in experimental mesocosms maintained under different pCO_2 levels. Mar. Ecol. Prog. Ser. 272: 25–31.

Sabine, C. L., and others. 2004. The oceanic sink for anthropogenic CO_2. Science 305:367–371.

Wanninkhof, R., E. Lewis, R. A. Feely, and F. J. Millero. 1999. The optimal carbonate dissociation constants for determining surface water pCO_2 from alkalinity and total inorganic carbon. Mar. Chem. 65:291-301.

Williams, P. J. le B., and J. K. Egge. 1998. The management and behavior of the mesocosms. Estuar. Coast. Shelf. S. 46 (Suppl. A):3–14.

Submitted 27 September 2007
Revised 5 December 2007
Accepted 30 December 2007